



HAL
open science

Terrestrial Carbonaceous Debris Tracing Atmospheric Hypervelocity-Shock Aeroplasma Processes

Marie-Agnès Courty, Jean-Michel Martinez

► **To cite this version:**

Marie-Agnès Courty, Jean-Michel Martinez. Terrestrial Carbonaceous Debris Tracing Atmospheric Hypervelocity-Shock Aeroplasma Processes. *Procedia Engineering*, 2015, 103, pp.81-88. 10.1016/j.proeng.2015.04.012 . hal-01175554

HAL Id: hal-01175554

<https://univ-perp.hal.science/hal-01175554>

Submitted on 10 Jul 2015

HAL is a multi-disciplinary open access archive for the deposit and dissemination of scientific research documents, whether they are published or not. The documents may come from teaching and research institutions in France or abroad, or from public or private research centers.

L'archive ouverte pluridisciplinaire **HAL**, est destinée au dépôt et à la diffusion de documents scientifiques de niveau recherche, publiés ou non, émanant des établissements d'enseignement et de recherche français ou étrangers, des laboratoires publics ou privés.



Distributed under a Creative Commons Attribution - NonCommercial - NoDerivatives 4.0 International License

The 13th Hypervelocity Impact Symposium**Terrestrial Carbonaceous Debris Tracing Atmospheric Hypervelocity-Shock
Aeroplasma Processes**Marie-Agnès Courty^{a*} and Jean-Michel Martinez^a^aUPR 8521 PROMES CNRS. Procédés et Matériaux Solaires. Tecnosud. 66100 Perpignan, France.**Abstract**

Atmospheric hypervelocity impacts are widely viewed to produce the meteoric smoke layer by the shock-less interactions of the impinging air molecules with the vaporized meteoroid. In contrast here, we intend to show how gas and solid aerosols when captured in the Mach cone of a bolide while entering the Earth atmosphere are transformed into a new range of polymeric nanomaterials. Carbonaceous materials from natural situations are studied from collect in a pilot region of Southern France in the following days of a high altitude meteor atmospheric airburst on 2011 August 2nd and since the 2013 February 15th Chelyabinsk meteoritic event in Ural. These materials are compared to the ones obtained by hypervelocity shock with the CEA Persephone light-gas gun. A numerical simulation with the Tycho software is performed to model the evolution of the increase of density directly in the rear front of the shockwave with the increase of velocity around an obstacle for high velocity inflow. The multidisciplinary approach reveals the production carbon-based nanosolids from terrestrial precursors by hypervelocity plasma particle deposition (HPPD) processes. The Tycho simulation helps to establish the lack of mixing between the ablation smoke and the surrounding atmosphere. The correlation between the simulation, the hypervelocity experiments and the natural situations shows the distinctive characteristics of visco-elastic filamentary nanosolids formed in the laminar domain of low pressure, the ones of nanoparticle-rich stiff film specific to the thin domain of high shear stress and the ones of dense glassy carbon with nanocarbon crystallites (graphite and graphene-like) only formed in the frontal high temperature and pressure domain. Data on the natural carbon-based nanosolids indicate that the atmospheric shock-dissociation occurred from a carbon pool dominated by dead atmospheric carbon. Diagnostic keys are provided to distinguish natural carbon-based nanosolids synthesized by HPPD just at the time of the hypervelocity atmospheric entry from their subsequent transformations during atmospheric transport by other aeroplasma processes.

© 2015 The Authors. Published by Elsevier Ltd. This is an open access article under the CC BY-NC-ND license (<http://creativecommons.org/licenses/by-nc-nd/4.0/>).

Peer-review under responsibility of the Curators of the University of Missouri On behalf of the Missouri University of Science and Technology

Keywords: hypervelocity; nanosolid; carbon; aerosol; plasma; shock-wave; simulation

1. Introduction

The 2013 February 15th Chelyabinsk has provided detailed observations on the serial high altitude airbursts when the hypervelocity bolide reached the oxygen-rich atmosphere [1] and the rapid dispersion of ablation debris across the Northern hemisphere [2]. Interactions of airburst products with atmospheric aerosols remain a challenging issue for defining the exact effects of past hypervelocity atmospheric entry from geological archives [3, 4].

* Marie-Agnès Courty. Tel.: 0468682734; fax: 0468682213.
E-mail address: marie-agnes.courty@promes.cnrs.fr

Theoretical calculations and laboratory experiments have shown the complexity of the physical processes that are initiated by hypervelocity entry in the earth atmosphere, known at first by massive vapor production issued from shock heating, but also by shear heating or microscopic localized heating [5, 6, 7]. Hypervelocity shocked-air organic synthesis is viewed to have yielded significant byproducts from chemical interactions by either the projectile matter or the atmospheric gas alone only under primitive atmosphere (e.g. CH₄-NH₃ rich) during the heavy bombardment period [8, 9]. In contrast, the more oxidizing atmosphere (e.g. CO₂-CO-N₂ dominant) that later established on Earth would not have provided the required conditions for abiotic chemical synthesis of organic matter [10, 6, 8]. Size of the impactor, its carbon content, and its velocity have been assumed to exert strong control on interactions between atmospheric gas and projectile material, particularly when forming CN radicals. Thus a significant production of "revive" organic carbon by hypervelocity-shock would only trace impacts by large carbonaceous colliders [8]. In contrast, we investigate here how new types of solid materials are synthesised by plasma processes from preexisting terrestrial precursors when captured in the Mach cone of a bolide entering the Earth atmosphere. The objective is to elucidating the close link between (1) initial atmospheric conditions, (2) intensity of the hypervelocity shock-wave and (3) characteristics of the produced carbonaceous materials. The study presents a comparison of air-formed carbonaceous materials from diverse natural situations to the ones from hypervelocity experiments, and a numerical simulations of the shock-wave propagation in the atmosphere.

2. Carbonaceous materials from natural situations

The study concerns a series of collect in a pilot region of Southern France that extends from the Mediterranean coast around Perpignan city, the Roussillon plain, the Eastern coastlands up to the Eastern Pyrennee mountains. The collect was initiated in August 2011 following an unusual debris fall with violent detonation that was reported to have occurred on a restricted area of the Pyrennee mountains 30 hours after the airburst of a hypervelocity meteor (34 km/s) at 30 km altitude in the same region. The marked increase in this region of unusual debris fall in the months following the 2013 February 15th Chelyabinsk meteoritic event in Ural has lead to a systematic survey of every aerosol fall at the finest spatial scale. All the solid debris have been extracted under the binocular microscope from water-sieving residues that range between a few mm down to 40 μm. The unusual debris have been classified -based on their colour, size, morphology, microstructure and abundance, and most particularly carbonaceous components. Scanning Electron Microscope and microprobe analyses (SEM-EDS) have been performed on a selection of fragments for each type of unusual debris to determine their composition and their microstructure down to nanoscales. The characterization has been completed by Transmission Electron Microscopy (TEM), Raman, spectrometry, X-ray mineralogy (XRD) and AMS ¹⁴C analysis.

Three depositional contexts of unusual debris which have never been described so far in present-day conditions have been identified based on the collect performed in the pilot region. Context A (Fig. 1a) corresponds to mm-thick debris layer traced throughout the pilot region. Their occurrence was noticed from April 2013 and is still going on. They are associated to short-term weak rains in the plain and a few cm snow fall in the mountains depending upon temperature conditions, and occasionally to regional-scale episodes of Saharan dust fall that are commonly encountered throughout the Northern Mediterranean basin. Besides the well known Saharan quartz grains, together with pollen grains, fine charcoal and marine aerosols, these regional debris layers are remarkable by the presence of two distinctive species: (Type 1) polymeric carbonaceous components formed of filaments, agglutinates and films (Fig. 1b, 1c, 1d, 1e, 1f); (Type 2) composite components formed of glassy carbon, magnetic spherules, breccia, and scoria-like clasts (Fig. 1g).

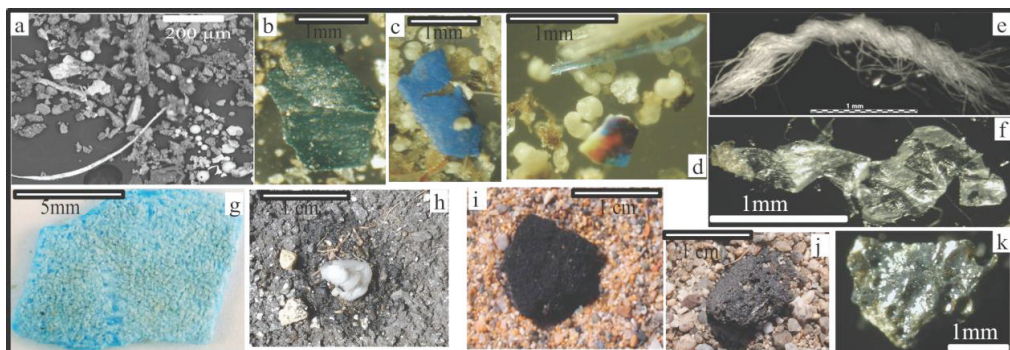


Fig. 1. Carbonaceous materials from natural situations: (a) Context A. SEM-BSE general view of particles from a debris layer dated on 2013 December 14th with carbonaceous filaments, glassy carbon and magnetite spherules. Context A: type 1 polymeric films (b, c, d, f) and filaments (d, e). Context C: (g) polymeric agglutinate and (h) polymeric blue film. Context B: type 2 (i) vesicular glassy carbon, (h) scoria-like granule and (g) vesicular blue glass.

Context B corresponds to cm-sized debris accumulations that have been traced at local spots along the Mediterranean coast plain. They also appeared in the pilot region from April 2013 and their fall is still going on. These depositional events were produced soon after (hours to days) violent thunderstorms with high altitude lightning strikes. The debris assemblage is formed of type 2 components (Fig. 1i, 1j, 1k) and hard polymeric agglutinates of various colors (Type 1b).

Context C corresponds to the unusual coarse debris fall reported on a small region of the Eastern Pyrenees mountains at the Angles village, soon after the high altitude meteor airburst in the same region, and to the local fall of fine debris along to violent hailstones locally recorded in the pilot region at the same time. The ca. 10 000 m² region that recorded a violent detonation and surface deflagration corresponds to the zone with high concentrations of type 1 and 2 debris, showing locally hard encrustation at the ground of type 1b polymeric components and visco-elastic agglutinates at the ground (Fig. 1g, 1h). Although part of the fine debris have been washed out by the subsequent hailstones, the local spatial survey has allowed to collect a diverse assemblage of coarse to fine type 1 components, associated to fine type 2 debris. Based on the long term collect in the pilot region, the debris fall of context C appears as an exceptional event by its depositional conditions and spatial pattern. Its assemblage shares compositional similarities to the ones from context A and B debris fall (Fig. 2).

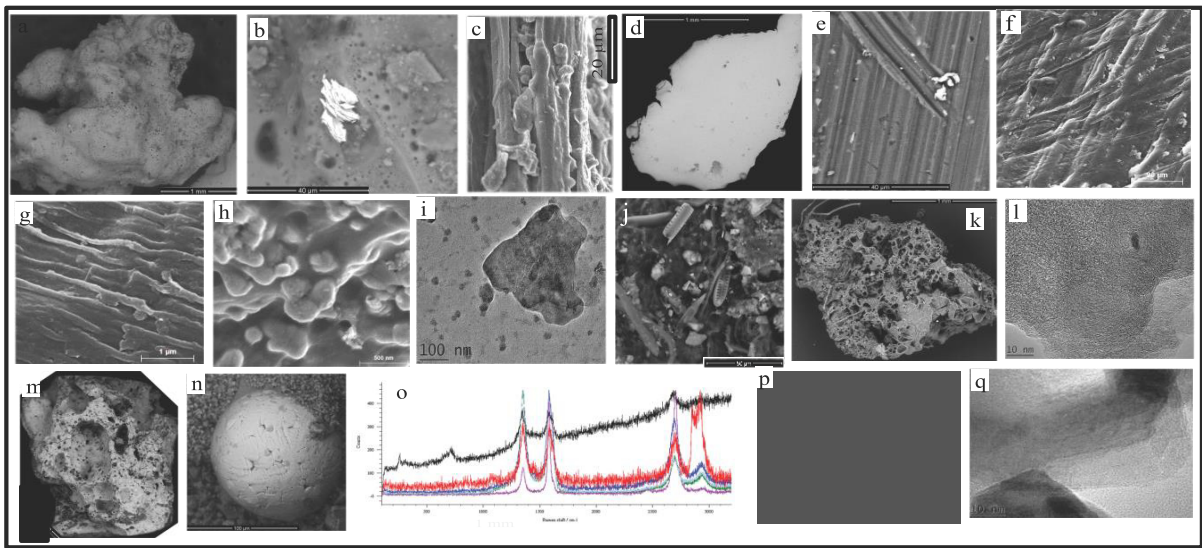


Fig. 2. Natural carbonaceous materials : (a & b) SEM-BSE view of a polymeric agglutinate (grey) with degassing vesicles, a Fe-Ni-Cr filamentary particle and silt at the surface (context C); (c) SEM-SE view showing the dense packing of nanostructured polymeric filaments; (d) micron-thick colored (yellow) polymeric film showing in (e) a dense packing of nanostructured polymeric filaments (context C); (f) SEM-SE view of 2f showing the superimposition of nanostructured polymeric filaments (context A); (g) SEM-SE view of 4e showing densely packed nanostructured polymeric filaments (context A); (h) SEM-SE view of 2g showing densely packed rounded nanoparticles embedded in a polymeric film; (i) TEM view of the polymeric blue film (2g) showing nanoparticle clusters consisting of metal, iron oxides and crystallized carbon; (j) SEM-BSE view of aerosols rich in marine diatoms embedded in a polymeric film; (k) SEM-SE view of vesicular glassy carbon (context C, type 2) with carbonaceous filaments and metal splash (Ag); (l) TEM view of (k) showing a typical onion-like nanostructure with crystallized carbon (black dot: 2.8 Å); (m) SEM-BSE view of a vesicular scoria-like breccia in polymeric filamentary carbon (context C, type 2); (n) SEM-BSE view of a magnetite spherule embedded in a scoria-like clast (Context C, type 2); (o) Raman spectra of a dense glassy carbon (cf. p) showing weakly graphitized carbon (black), graphite (purple; blue, green) and graphene-like carbon (red); (p) SEM-BSE view of a dense glassy carbon with splash of Ag nanoparticles in bright (context C, type 2); (q) TEM view of the densely packed graphitic filaments.

This comprises: (a) silt to sand-sized aerosols (marine microorganisms, quartz, spherules) embedded in a filamentary polymeric matrix, common to type 1 or 2 components (Fig. 2a, 2b, 2j); (b) a vesicular pattern typical of degassing before solidification (Fig. 1g, 1h, 1i, 2b, 2k, 2n); (c) a densely packed nanostructured pattern encountered for all the type 1 polymeric components, either as subparallel nanofilaments for the visco-elastic ones or as nanospheres for the stiffer ones (Fig. 2e, 2f, 2g, 2h); (d) randomly distributed metal and oxide nanoparticles with rare clusters in the matrix of the stiffer type 1 polymeric components (Fig. 2i); (e) brittle vesicular glassy carbon formed of densely packed nanoparticles with rare crystallized carbon (Fig. 2l). In contrast, hard, vesicular glassy carbon with a composite matrix formed of densely packed

graphite and graphene-like nanofilaments has only been observed in the fine debris collected from the local hailstones of context C (Fig. 2o, 2p, 2q). Moreover, type 2 and 1 components from the three contexts studied show the occurrence of nanostructured ribbon-shaped metals adherant to their surface of variable nature (Fe-Cr, Fe-Cr-Ni, Cu-Zn, Al) and metal micro agglutinates of Au, Ag, Au-Pt (Fig. 2b, 2e, 2q). The metal nanoparticles within the type 1 polymeric matrix also dominantly consist of these elements, together with the common occurrence of Pb and Ti oxides (Fig. 2i).

XRD analysis shows that the polymeric components encountered in the three contexts consist mostly of crystallized to amorphous n-paraffin wax (CH₂)_x and occasionally of other types (i.e. Quinacridone: C₂OH₁₂N₂O₂). Based on multi-step heating from 100 to 1300 °C and by comparison with industrial paraffin, the visco-elastic white one appears to derive from an acetylene precursor, while the stiffer blue one is derived from a polyethylene one. The ¹³C values of the different carbonaceous materials are in the range of terrestrial precursors. The AMS ¹⁴C dating indicates that most of the polymeric components and dense glassy carbon are derived from dead carbon, except a slightly younger ¹⁴C age for the context C white polymeric agglutinates. These values contrast with the modern age obtained on the brittle black glassy carbon of the context C. The context A AMS ¹⁴C dating shows consistent results between the modern age of fine charcoal and white filaments that are not nanostructured and mixed precursors of different ages for the nanostructured ones.

3. Carbonaceous materials from hypervelocity experiments

The data used here refers to a series of collisions which have been performed at the CEA Gramat Center (France) with the hypervelocity Persephone light-gas gun. The experiment was originally designed for defense purposes in order to refine the calibration of code when calculating the impact of hypervelocity steel projectile at speed from 4.1 to 7.9 km/s on a 40 mm thick aluminium target. The interest of this experiment lies in the use of a particular equipment formed of two carbon-based elements (polycarbonate and polystyrene pieces (cf. Fig. 3) which was designed to separate the steel projectile from the launching support just before the impact. The two-carbon-based elements are vaporized during the launching, generating a cloud of black carbon throughout the launching chamber. The impact craters have revealed polymeric materials in the inner part of the impact crater and in cracks at its periphery (Fig. 4a). Considering the temperature (a few hundred degrees) and pressure (a few tens Mpa) at the moment of impact, the polymeric materials appear to have been synthesised from the carbon-rich vapor soon after the collision. In situ analysis of the carbonaceous materials in the sectioned impact craters for the Persephone experiments has been performed using a large chamber environmental SEM.

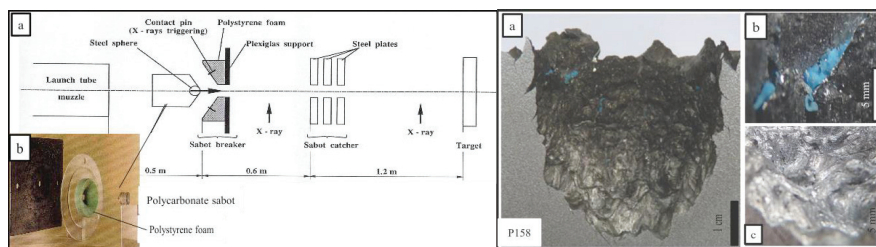


Figure 3 (left). The Persephone hypervelocity light-gun gas : (a) diagram of the sabot/projectile separation by the impact technique. (b) view of the single piece sabot, sabot breaker and recover catcher plate.

Fig. 4 (right). Carbonaceous materials from hypervelocity experiments : (a) Impact crater at 7 km/s; (b) blue carbonaceous blocky mass trapped in the crater cracks; (c) pinkish carbonaceous coating on the crater bottom.

The impact craters show a marked contrast between the carbonaceous materials in the cracks and the one coating the crater wall (Fig. 4b, 4c). The later appears pale pink to dark grey, firmly adherent to the aluminium support and resistant to the laser or electron beam even at high power. The great structural and compositional heterogeneities at microscales of the polymeric domains express mixing of metal particles from the steel projectile (iron spherules and Fe-Cr-Ni flakes) and from the aluminium target (Fig. 5a, 5b, 5h, 5i). The co-existence at micron size of different graphitic and graphene like crystallized carbon within an amorphous polymeric matrix with dominant CH-based components is confirmed by Raman spectrometry (Fig. 5l). The carbonaceous filaments in the cracks are of two types: (a) a visco-elastic, white, filamentary nanostructured material, nearly without non-carbon nanoparticles, with abundant degassing fine vesicles; it is trapped in the deepest part of the cracks (Fig. 5c & 5d); (b) a slightly stiffer blue materials formed of densely packed nanospherules with metal and oxide particles deriving only from the steel projectile (Fe, Fe-Cr, Fe-Cr-Ni). Instability of the white polymer under the laser or electron beam has not allowed to obtain TEM or Raman data. Better stability of the blue material under the electron beam has allowed to recognize the irregular distribution of the metal and oxide nanoparticles in the amorphous polymeric matrix and the rare occurrence of crystallized carbon nanodomains (Fig. 5i, 5j).

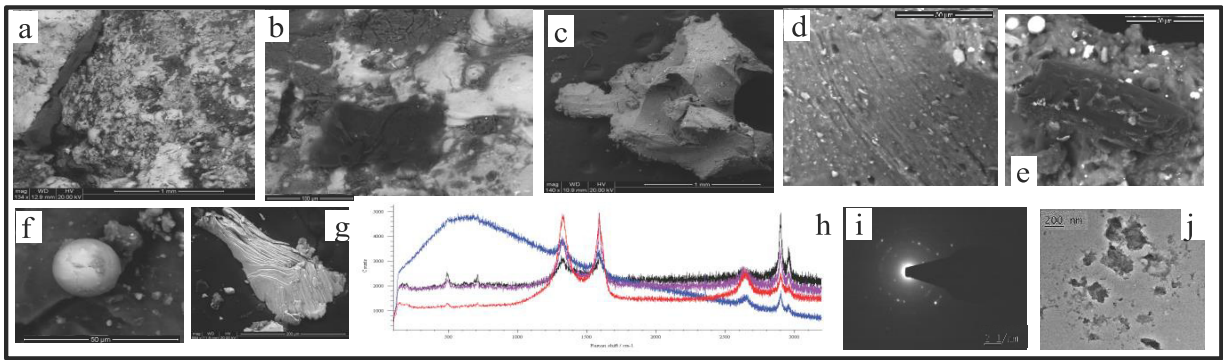


Fig. 5. Characteristics of the carbonaceous materials from hypervelocity experiments : (a) SEM-BSE view of the blue polymeric mass in the cracks; (b) SEM-BSE view of the pinkish polymeric coating on the impact crater, partly covered by the white filamentary polymer; (c & d) SEM-BSE view of the elastic filamentary white polymer showing degassing fine vesicles; (e) SEM-BSE of the polymeric nanostructured fine mass sprinkled by metal spherules; (f & g) SEM-BSE views of a magnetite spherule (f) and of a Fe-Ni-Cr filamentary particle (g) derived from the steel projectile and trapped in the polymeric matrix; (h) Raman spectra from the carbonaceous coating on the crater showing the close imbrication of amorphous carbon (blue), graphene-like carbon (red) and crystallized polymers (purple and black); (i) diffraction diagram of a crystallized carbon nanodomain; (j) TEM view of the blue polymeric mass with metal and iron oxide nanoparticles.

4. Numerical simulation

A numerical simulation has been performed to model the evolution of the spatio-temporal density around an obstacle for high velocity inflow. Our main interest has been to correlate the increase of density directly in the rear front of the shockwave with the increase of velocity. The numerical simulation has been performed using the free software Tycho-cfd (Tyrolean Computational Hydrodynamics), which is a multidimensional compressible hydrodynamic code fully parallelized. The system simulated is a bidimensional channel with a circular obstacle. The coordinates are cartesian and the size of the domain is 2x4 m height and width. The ablation during the arrival on the atmosphere is not taken into account. We assume that our body is perfectly circular and has gained during its entry in the atmosphere a temperature of 2000°K. Due to high inflow velocity, the gravity is neglected. In the same way, the viscosity of the fluid around the body is neglected too. The gas around the bolide is a mixture of air and aerosols, including gas and nanoparticles, the density is supposed to be more less equivalent to the one of air with an imposed constant value independent of altitude.

The evolution of the velocity flow through time is made until the position of the generated shockwave in front of the bolide is stable. Several simulations have been done depending on different inflow velocity field from 1 to 30 km.s⁻¹.

The first simulation (Fig. 6) shows the density map of mixture around the bolide for a velocity inflow imposed to 10 km.s⁻¹ in a Lagrangian point of view. The velocity field is superimposed to the density map and a zooming area is presented to enhance the visibility around the shockwave. The red area is highlighting the increase of density in the rear of the shockwave and shows the relaxation of density over several meter behind it. The velocity field is separated into three big domains: the domain 1 is representing the inflow field which is, by definition, totally laminar; the domain 2 is directly issued from the shock-wave and presents a laminar flow field totally independent from the drag of the bolide; the domain 3 presents a turbulent flow channeled in a tube limited by the size of the bolide. The lack of mixing between ablation smoke and aerosols in the atmosphere is clearly marked by the sharp boundary between domains 2 and 3 (Fig. 7a). The zoomed area that focuses on the abrupt change of direction of the velocities, directly linked to the increase of pressure and temperature emphasizes the key zone of shear stress. The evolution of density along an horizontal line at a distance of one meter from the bolide is reported (Fig. 7b) for several inflow velocities. The position of the shockwave is depending on the inflow velocity and is clearly linked with the angle of the shockwave with the horizontal. The relaxation rate to equilibrium is also increasing with the inflow velocity until a threshold plateau is achieved. This suggests that there is no change in the evolution of the velocity field over 10 km.s⁻¹ except for the magnitude of the velocities, pressures and temperatures. The maxima of each density curve have been reported in a curve (Fig. 7c) to present the threshold of density over 10 km.s⁻¹. This means that the gases are obeying to perfect gas law as commonly accepted.

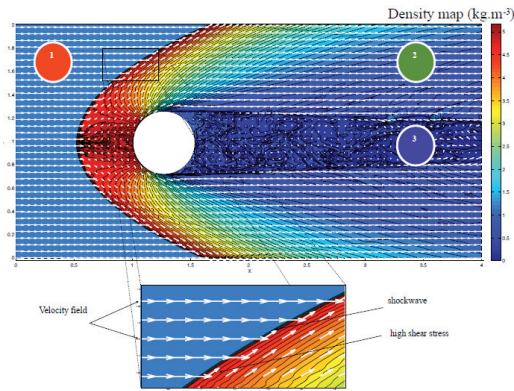


Fig. 6. Density map and flow field around a circular body for a 10 km/s inflow velocity

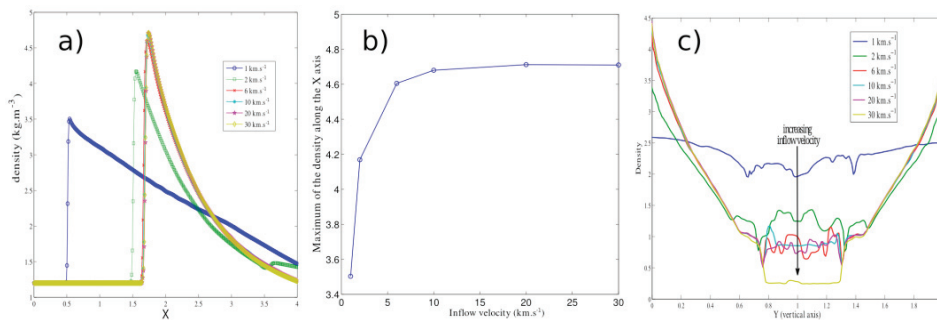


Fig. 7a . Evolution of density along the vertical axis at the middle of the whole domain. Fig. 7b. Density evolution over an horizontal line at 1m up of the bolide. Fig. 7c. Evolution of maximum density relative to inflow velocity

5. Discussion

The Persephone experiments bring three major interpretation:

- The thermal plasma produced by the shock disintegration of the carbon-based elements has resulted into the total dissociation of the polymers and molecules.
- The synthesis of new polymeric materials, defined by their properties as nanosolids, is thus viewed to have formed from densification of the thermal plasma by the shock-wave that rebounded from the collision.
- The long distance between the sabot-breaker and the target explains the lack of mixing between carbon-based shocked plasma with the high pressure and high temperature of the collisional plasma .

The pattern, the structural and compositional variability of the polymeric nanosolids are interpreted to reflect a three-step plasma process : (Step 1) hypervelocity deposition on the hot crater walls of the pinkish graphitic and graphene-like filamentary coatings and individual filaments; (Step 2) deposition at lower speed and reduced temperature of the nanoparticle-free, volatile-rich, vapour condensates trapped in the deep crater cracks and formation of highly oriented polymer fibers along the crater walls; (Step 3) final filling of the crater cracks with a denser polymeric material due to the increasing production of nanoparticles behind the rebound shockwave in agreement with knowledge on shock-produced nanoparticles [11]. The multi-step process of carbon-based nanosolids described here thus appears

to correspond to the well known hypersonic plasma particle deposition [12, 13], and now defined here as hypervelocity plasma particle deposition (HPPD). The structural and compositional resemblance between the carbon-based nanosolids of the Persephone experiments and the type 1 carbonaceous nanomaterials encountered in the natural situations incite to consider their synthesis by a similar process. The atmospheric terrestrial aerosol precursors can be viewed as the equivalent of the dissociated carbon-based elements. This interpretation is supported by the identification of acetylene and polyethylene precursors for the carbon-based nanosolids which trace preferential production of small polymeric chains by the shock-wave in agreement with knowledge on shock polymerization process [14]. Similarly to the Persephone experiment, the shock-wave created by hypervelocity entry in the earth atmosphere is thus interpreted to produce carbon-based nanosolids from the shock-dissociated aerosols. Terrestrial signatures of the neoformed nanosolids without evidence

of mixing with ablation products can be explained by the Tycho simulation. The later emphasizes the lack of mixing between the ablation smoke and the surrounding atmosphere, and furthermore reveals the formation of a channel with sharp boundary between two domains: (1) the inner part (domain 3) consisting of the turbulent ablated smoke; (2) outside, the laminar surrounding atmosphere (domains 1 & 2). Based on the Tycho simulation and with the help of the Persephone experiments, a correlation can be tentatively established between the two types of laminar regimes in the surrounding atmosphere and the two types of polymeric nanosolids encountered in the natural situations. The visco-elastic filamentary ones with diluted nanoparticles and evidence of degasing would be produced along the laminar atmospheric domain of low pressure (domain 2). In contrast, the stiffer film with a dense network of nanoparticles would only have formed within the thin high shear stress domain (domain 1). In addition, the confrontation of the Persephone experiment and the Tycho simulation suggests that the type 2 dense glassy carbon with nanocarbon crystallites (graphite and graphene-like) would only be produced in the frontal domain 2 marked by the highest temperature and pressure.

The three classes of carbon-based nanosolids formed by HPPD allow to clarify the forming processes of the similar ones from the natural situations encountered in the pilot region. The occurrence on a restricted area of carbonaceous materials mostly formed of HPPD carbon-based nanosolids for the context C suggests that this debris fall is directly linked to the hypervelocity meteor entry which occurred 30 hours before in the same region. The mixing of the visco-elastic nanosolids with intact aerosols shows that the aggregation process has been continuing after the passage of the shock wave. This would reflect a transitional stage of low pressure plasma due to large scale ionization by the shock-wave with considerable production of electrons. These conditions could easily induce small electric discharge and lightning strikes, thus resulting in the production of thermal plasma. Most of the type 2 components from the context C would have formed by these indirect effects, except the dense glassy carbon. The appearance of context A debris fall in the months following the 2013 February 15th Chelyabinsk meteoritic event in Ural in the pilot region incites to envisage a direct link between the two phenomena. The regional occurrence of HPPD carbon-based nanosolids in every debris fall, their fragmented aspect and their fine mixing to a large diversity of usual aerosols strongly contrasts from the context C record. Thus, they cannot be viewed as HPPD products from occasional meteor entry that would have occurred in the region but more likely as components of long distance aerosol transport. This interpretation would be rather consistent with the rapid hemispheric dispersion of the ablation smoke from the Chelyabinsk event that has been observed [2]. It implies that the HPPD carbon-based nanosolids formed by this event would have also been transported across vast regions. The context B debris falls do not bear the diagnostic attributes of HPPD carbon-based nanosolids but more likely the ones produced by other kinds of atmospheric plasma, particularly the thermal one due to lightning strikes. The abundance of blocky polymeric nanomaterials rather different from the HPPD ones suggests that they might have formed from other kinds of hypervelocity process in electrically charged dusty clouds along to violent thunderstorms. The similar morphology of the metal flakes encountered in the three contexts and their strong adhesion at the surface of type 1 or 2 components suggest that also formed by hot thermal splash, also most likely in electrically charged dusty clouds.

The carbon isotopic data of the HPPD carbon-based nanosolids indicate that the atmospheric shock-dissociation occurred from a carbon pool dominated by dead carbon, and most likely originally consisting of CH₄ as suggested by the evidence of acetylene and polyethylene precursors for the type 1 polymeric nanosolids. The compositional range of metal and oxide nanoparticles in the polymeric matrix seems to be consistent with CH₄ of volcanic origin. In contrast, type 1 and 2 compounds would form from atmospheric CO₂ or from recent black carbon of biomass firing origin that is known to be a potential carbon sink in the atmosphere [15]. This suggests that the precursor carbon of the HPPD nanosolids would rather originate from erratic pools of solid phases that could have been stored for long time period at high altitude [16]. In mixed debris assemblage, the amount and nature of aerosols that are involved in the production of type 2 components appears to offer a signature of the atmospheric conditions at the time of the hypervelocity entry and during the following months. Further investigations should help elucidating how far the production of type 2 compounds since the Chelyabinsk event could reflect anthropic increase of atmospheric dust loading along to other natural sources (volcanism, storms, wildfires).

6. Conclusions

The integrated study of puzzling carbonaceous materials encountered in natural situations with investigations on resembling polymeric components formed by hypervelocity experiments has helped, with the assistance of numerical simulation, to providing a novative research hypothesis. Bolide entry in the atmosphere is concluded to produce carbon-based nanosolids from terrestrial precursors by hypervelocity plasma particle deposition (HPPD) processes. The multidisciplinary approach has provided the diagnostic keys to distinguish in natural situations carbon-based nanosolids synthesised by HPPD just at the time of the hypervelocity atmospheric entry and the subsequent composite materials later produced during the atmospheric transport by complex aeroplasma processes. This challenging perspective should greatly help to further reveal periods of intense aeroplasma activities marked by complex plasma-formed debris assemblage in geological records, particularly the ones related to impact events. In addition, air-formed solid products consolidated by shock-waves from

volcanic eruptions could also be detected. The evidence for the lack of mixing between the neofomed terrestrial nanosolids and ablation smoke emphasizes that components from any extra-terrestrial colliders would not contribute to the formation of impact-linked HPPD debris layers. In contrast, the study reveals the critical role of hypothetical sporadic dead-carbon pools present in the upper atmosphere on the production of HPPD carbon-based nanosolids, the exact nature of which yet remains to be further investigated.

The tycho numerical simulation used here is limited by its inability to taking into account transformation by the shock-wave of the original precursors in the earth atmosphere. A refined study of nanoparticle production from preexisting aerosols using adapted codes would greatly help understanding the puzzling selective formation of CH-based nanosolids.

Certain structural patterns of the filamentary nanosolids suggest a possible interference of multiple shock waves during their synthesis. Further development of the tycho numerical simulation could help to take into account the interactions between the bolide shock-wave with the ones produced by the airburst which might play a key role on the nanosolid production.

Acknowledgements

We are greatly indebted to Marc Sibeaud and Alain Cayrol (CEA Gramat) at the Direction of Military Applications, CEA Gramat Center (France) for offering access to the Persephone Light gas gun experiments. We thank Magali Michel, Michaël Vaillant and Brigitte Deniaux for their assistance in the field survey of the 2011 August 3rd debris fall. Guispert Guirardo and Mercè Moncusi at the SRICT-Tarragona university are acknowledged for their technical assistance. We thank Sylvie Bonnamy and Fabienne Warmont at the CRMD-Orleans university for the TEM analysis and Dimitri Gorand at the C2M-Perpignan university for the SEM analysis. We thank Wolfgang Kapferer for the implementation of the tycho cfd-software.

References

- [1] Popova, O.P. et al. Chelyabinsk Airburst Consortium , 2013. Chelyabinsk airburst, damage assessment, meteorite recovery, and characterization. *Science*, 342 (6162), pp.1069-73
- [2] Gorkavyi, N., Rault, D. F. , Newman, P. A., da Silva, A. M., Dudorov, A. E., 2013. New stratospheric dust belt due to the Chelyabinsk bolide. *Geophysical Research Letters* 40 (17), pp. 4728–4733.
- [3] O’Keefe, J. D., Ahrens, T. J., 1982. Impact ejecta dynamics in an atmosphere: Experimental results and extrapolations, in "Geologic Implications of Impacts of Large Asteroids and Comets on the Earth", L. Silver and P. H. Schultz, Editor, Special Paper Geological Society of America, 190, pp. 103– 120.
- [4] Schultz, P. H., and Gault, D. E., 1990. Prolonged global catastrophes from oblique impact, in *Global Catastrophes in Earth History: An Interdisciplinary Conference on Impacts, Volcanism, and Mass Mortality*, V. L. Sharpton and P. D. Ward, editor, *Spec. Pap. Geol. Soc. Am.*, 247, pp. 239– 261.
- [5] Ahrens, T. J., O’Keefe, J. D., 1983. Impact of an asteroid or comet in the ocean and extinction of terrestrial life., *Journal of Geophysical Research*, 88(S02), A799–A806.
- [6] Fegley, B., Prinn, Jr., R. G., Hartman, H., Watkins, G. H., 1986. Chemical effects on large impacts on the Earth’s primitive atmosphere, *Nature*, 319, pp. 305– 308.
- [7] Sugita, S., Schultz, P. H., 2003. Interaction between impact-induced vapor clouds and the ambient atmosphere: 2. Theoretical modeling, *Journal of Geophysical Research*, 108 (E6), p. 5052.
- [8] Chyba, C., Sagan, C., 1992. Endogenous production, exogenous delivery and impact-shock synthesis of organic molecules: an inventory for the origins of life, *Nature* 355, pp.125 - 132
- [9] Sugita, S., Schultz, P. H., 2009. Efficient cyanide formation due to impacts of carbonaceous bodies on a planet with a nitrogen-rich atmosphere. *Geophysical Research Letters* 36, L20204.
- [10] Walker, W.L., Chameides, W.L., 1981. Rates of fixation by lightning of carbon and nitrogen in possible primitive atmospheres. *Origins of life*, 11, pp. 285-302.
- [11] Rao, N. P. et al. 1998. Hypersonic plasma particle deposition of nanostructured silicon and silicon carbide. *Journal of Aerosol Science* 29, pp.707-720.
- [12] Hafiz, J. et al. 2006. Hypersonic plasma particle deposition - A hybrid between plasma spraying and vapor deposition. *Journal of Thermal Spray Technology* 15(4), pp. 822-826.
- [13] Eremin, A. V., 2013. A new model for carbon nanoparticle formation in the pyrolysis process behind shock waves. *High Temperature*, 51 (5), pp. 673-680.
- [14] Dremin, A. and Babare, L., 1984. On the shock polymerization process. *Journal de Physique. Colloques*, 45 (C8), pp. C8-177-C8-186.
- [15] Ball, R., 2008. Combustion of Biomass as a Global Carbon Sink. *The Open Thermodynamics Journal* (2), pp. 106-108.
- [16] Dzyuba, A. V., Eliseev, A. V., and Mokhov, I. I., 2012. Estimates of Changes in the Rate of Methane Sink from the Atmosphere under Climate Warming. *Izvestiya, Atmospheric and Oceanic Physics*, 2012, Vol. 48, No. 3, pp. 332–342.